DEVELOPMENTAL BIOLOGY **191,** 103–117 (1997)
ARTICLE NO. DB978707

GFP-Moesin Illuminates Actin Cytoskeleton Dynamics in Living Tissue and Demonstrates Cell Shape Changes during Morphogenesis in *Drosophila*

Kevin A. Edwards,[1] Maddy Demsky, Ruth A. Montague, Nate Weymouth, and Daniel P. Kiehart[2]

Department of Cell Biology, Duke University Medical Center, Durham, North Carolina 27710

Moesin, ezrin, and radixin (MER) are components of the cortical actin cytoskeleton and membrane processes such as filopodia and microvilli. Their C-terminal tails contain an extended region that is predicted to be helical, an actin binding domain, and a region(s) that participates in self-association. We engineered an *in vivo* fluorescent actin binding protein (GFP-moe) by joining sequences that encode the jellyfish green fluorescent protein (GFP) to sequences that encode the C-terminal end of the sole *Drosophila* MER homolog, moesin [*Moesin-like* gene product, referred to previously as the D17 MER-like protein; Edwards *et al.*, 1994, *Proc. Natl. Acad. Sci. USA* 91, 4589], and *Dmoesin* [McCartney and Fehon, 1996, *J. Cell Biol.* 133, 843]. Transgenic flies expressing this fusion protein under control of the *hsp70* promoter were generated and used for analysis of cell shape changes during morphogenesis of various developmental stages and tissues. Following heat shock, high levels of stable fusion protein are produced by all somatic tissues. GFP-moe localizes to the cortical actin cytoskeleton, providing a strong *in vivo* marker for cell shape and pattern during epithelial morphogenesis. The protein also becomes highly enriched in pseudopods, microvilli, axons, denticles, the border cell process, and other membrane projections, potentially by binding to endogenous moesin as well as actin. We show that GFP-moe can be used to examine the development and behavior of these dynamic structures in live specimens. We observe a bright green fluorescent, presumably actin-rich, polar cell proboscis that inserts itself into the forming micropyle and appears to maintain an opening for sperm passage around which the chorion is formed. We also confirm the existence of an actin-rich purse string at the leading edge of the lateral epidermis and provide a dynamic analysis of its behavior as it migrates during dorsal closure. Observations of embryos, larvae, and pupae show that GFP-moe is also useful for labeling the developing nervous system and will be a good general marker of dynamic cell behavior during morphogenesis in live tissues and demonstrate that fusion of a subcellular localization signal to GFP greatly increases its utility as a cell marker.

INTRODUCTION

Drosophila has become a powerful model organism for the study of morphogenesis. Scores of genes involved in the specification of cell fate have been identified, and numerous recent studies have focused on the effector molecules that carry out these fates (e.g., Young *et al.*, 1993; Mahajan-Miklos and Cooley, 1994; von Kalm *et al.*, 1995; Edwards and Kiehart, 1996). Because many of these developmentally important molecules are also essential components of the cell, mutations that eliminate them can lead to complex phenotypes that obscure their functions.

Several new molecular genetic techniques can facilitate the analysis of proteins with complex mutant phenotypes. By exploiting the yeast transcriptional regulator GAL4, Brand *et al.* (1994) devised a system that allows exogenous genes to be specifically expressed in nearly any desired cell or tissue type in *Drosophila.* Golic and Lindquist (1989) imported a yeast recombinase gene and its target sequences (the *FLP/FRT* system) into flies, allowing a gene product to be efficiently eliminated in small, random patches of cells (Xu and Rubin, 1993). These methods permit the controlled expression of mutant phenotypes. Judicious use of another imported molecule, green fluorescent protein (GFP), can

[1] Current address: Center for Conservation Research and Training, University of Hawaii, Honolulu, HI 96822.

[2] To whom correspondence should be addressed. Fax: (919) 684-5481. E-mail: D. Kiehart@Collbio.Duke.edu.

0012-1606/97 $25.00

complement these approaches by allowing phenotypes to be examined at the cellular and subcellular levels in living specimens.

GFP acts at the final step in the bioluminescent pathway of the jellyfish *Aequorea victoria* (a pathway that also includes the calcium indicator aequorin). Blue light excites the protein's chromophore, derived from a Ser-Tyr-Gly tripeptide in its sequence, causing it to emit green light (Prasher *et al.*, 1992; Cody *et al.*, 1993). Since the chromophore forms autocatalytically upon expression of the protein, and its fluorescence is highly stable and compatible with standard optics used to image fluorescein, GFP has rapidly gained popularity as a protein tag and cytoplasmic tracer dye (Steams, 1995). GFP was first expressed exogenously in *Escherichia coli* and then in specific *Caenorhabditis elegans* neurons, where it diffuses throughout the cell and labels long axonal processes (Chalfie *et al.*, 1994).

GFP has been fused to a number of fly proteins where it acts as a benign tag. Wang and Hazelrigg (1994) fused GFP to Exuperantia (Exu), which is involved in cytoplasmic RNA localization in *Drosophila*. A transgene bearing the *exu-GFP* fusion produces a protein that mimics the distribution of endogenous Exu as determined by immunofluorescence. Even more importantly, the transgene rescues flies with a null mutation in *exu*, proving that the 27-kDa GFP moiety does not interfere with normal Exu function. In rescued flies, GFP distribution represents all Exu in the cell, and every such fly is automatically labeled. These features make transgenic GFP a major technical advance over comparable methods such as immunofluorescence and microinjection of fluorescently labeled proteins. Moreover, the dynamic behavior of GFP-Exu in the developing *Drosophila* egg chamber has been analyzed by time-lapse video microscopy, a major achievement in the *in vivo* analysis of protein function (Theurkauf and Hazelrigg, personal communication). Similarly, Endow and Komma (1996) fused GFP to both wild-type and mutant forms of the Ncd microtubule motor protein and then followed Ncd dynamics to show cell cycle-dependent localization of the protein to centrosomes and spindles that was aberrant in the mutant constructs. Other examples of the use of GFP in fly include Kerrebrock and colleagues (1995) who used a GFP fusion to study Mei-S332, a protein required for sister-chromatid cohesion and Micklem and colleagues (1997) who used two different GFP constructs to analyze the distribution of microtubules and their polarity in egg chambers.

In *Drosophila* GFP has also been used as a cell- and organelle-specific marker. Yeh *et al.* (1995) constructed a GAL4-inducible GFP responder gene. A specific cell type can be made to fluoresce by crossing flies carrying the GFP responder to flies with the desired tissue-specific GAL4 expression. In our hands, this system works well for some, but not all, GAL4 lines and the resulting fluorescence can be somewhat dim because expressed GFP is diffuse within the cell. Davis *et al.* (1995) and Shiga *et al.* (1996) made nuclear GFP constructs and used them to monitor gene expression and morphogenesis. In each case the authors had some difficulty in imaging the GFP fusions that were expressed by their constructs. Barthmaier and Fyrberg (1995) drove high-level GFP expression with the *Act88F* promoter, providing a specific (though still diffuse) marker for indirect flight muscle cells. Similarly, Plautz *et al.* (1996) expressed GFP specifically in photoreceptors using *glass*-responsive regulatory sequences and Potter *et al.* (1996) used two-photon laser-scanning confocal microscopy to image GFP expressed under the control of an eye-specific promoter.

In *Saccharomyces cerevisiae* and *Dictyostelium*, GFP has been used to image the actin cytoskeleton through fusions to actin and to actin binding proteins (Doyle and Botstein, 1996; Waddle *et al.*, 1996; Westphal *et al.*, 1997). In these cases, the ability to image the cytoskeleton in living cells has allowed analysis of cellular dynamics not easily appreciated in series of fixed and stained specimens.

We have generated flies that can express a fusion protein consisting of GFP attached to a portion of moesin (see below) that includes its actin binding domain. Moesin's association with actin makes this fusion protein useful as an *in vivo* label for the cell cortex and other actin-rich structures in living animals, cells, and tissues.

Drosophila moesin was identified by expression cloning in the fission yeast *Schizosaccharomyces pombe* (Edwards *et al.*, 1994) and by a polymerase chain reaction screen for MER proteins (McCartney and Fehon, 1996). In the expression screen, a *Drosophila* cDNA library in an inducible expression vector was transformed into yeast cells, and a cDNA encoding the C-terminal half of moesin (''moesin tail'') was recovered because it strongly disrupts yeast cytokinesis and cell shape when overexpressed. In these overexpressing cells, both actin and the moesin tail fragment become concentrated at the plasma membrane; this sequestration of actin can account for the defective cell growth phenotype (Edwards *et al.*, 1994, and unpublished).

Moesin is a member of an extended family of putative membrane–cytoskeleton linker proteins that concentrate in the cortical actin cytoskeleton and actin-based cell surface projections such as filopodia (Furthmayr *et al.*, 1992; Algrain *et al.*, 1993; Franck *et al.*, 1993; Amieva and Furthmayr, 1995). It is highly similar to and nearly collinear with ezrin and radixin (''MER'' or ''ERM'' proteins; see alignment in Edwards *et al.*, 1994). *Drosophila* appears to have only a single homolog of these three closely related membrane skeletal proteins (McCartney and Fehon, 1996). The sequence of this homolog is nominally more similar to vertebrate moesins than ezrins or radixins, so we refer to it as moesin (see also section on nomenclature under Materials and Methods).

The N-terminal ''head'' domain of these proteins is also conserved in merlin, protein 4.1, talin, and several other proteins, each of which has a distinct tail domain (Arpin *et al.*, 1994). The conserved head domain is thought to bind to the plasma membrane through the cytoplasmic tail of transmembrane proteins such as CD44 (Tsukita *et al.*, 1994). The tail domain of ezrin can directly bind both F-actin and other molecules of ezrin or moesin (Turunen *et al.*, 1994; Gary and Bretscher, 1995). The F-actin binding region of the tail is well conserved among ezrin, radixin,

and moesin proteins from several phyla. Interactions between the head and tail have been suggested to mask the actin binding site under certain conditions (Gary and Bretscher, 1995; Berryman *et al.*, 1995). Phosphorylation of the MER tail, at both tyrosine and threonine residues that are conserved in *Drosophila*, has been implicated as a regulatory step lying between cell activation and cell shape change (e.g., A431 tumor cell stimulation by EGF: Krieg and Hunter, 1992; platelet activation by thrombin: Nakamura *et al.*, 1995).

We expected one of two possible outcomes from expressing the GFP-moesin tail fusion in *Drosophila*. The fusion could disrupt the actin cytoskeleton in a way that would cause a visible phenotype (as might be expected from the expression of the larger moesin fragment in *S. pombe*). The phenotype might then be employed in genetic modifier screens to identify moesin-interacting or cytoskeletal proteins. Alternatively, the GFP-moe could colocalize with actin without causing a phenotype. We observed the latter result: even continuous presence of the fusion protein has little or no deleterious effect on the animal. The fusion protein is, however, very effective as a vital marker for observing a variety of actin-based structures throughout development.

MATERIALS AND METHODS

Plasmid construction. An *hsp70* promoter-driven GFP-moesin cDNA fusion (*P*[w^+, *hs-GFP-moe*], referred to as *hs-GFP-moe*) was produced in the *P* element germline transformation vector pCaSpeR-hs (Thummel and Pirotta, 1992; see Lindsley and Zimm, 1992, for genetic nomenclature). Two fragments were ligated into *Eco*RI–*Not*I cut pCaSpeR-hs as follows. The 5′ fragment was PCR-amplified from a wild-type GFP cDNA (pGFP10.1, Chalfie *et al.*, 1994) using primers GFP-EX-f (5′-cagaattctagaaaaatgagtaaaggagaagaac) and GFP-H3-r (5′-gattaaagcttgtatagttcatccatgcc) and then digested with *Eco*RI and *Hin*dIII. GFP-H3-r introduces a *Hin*dIII site in frame with the GFP cDNA, replacing the stop codon with a Leu codon. The 3′ fragment was PCR amplified from pREP-D17 partial moesin cDNA (Edwards *et al.*, 1994) using primers D17-HC-f (5′-gccgcaagcttgacaccatcgatgtgca) and Pom1-r (5′-tgggcttccatagtttgaaag) and then digested with *Not*I and *Hin*dIII. D17-HC-f introduces a *Hin*dIII site in frame with the moesin cDNA just 5′ of the DTIDV coding region at the beginning of the α helical tail. The *Not*I site lies at the end of the moesin cDNA so that the digested fragment includes the natural moesin stop codon and 3′ untranslated region. Ligation results in a fused coding region that replaces the conserved globular head region of moesin with full-length GFP. The sequence at the junction is DELYK***L***DTIDV (DELYK is the normal C-terminus of GFP, the ***L*** is the only amino acid that was not in either of the original sequences, and DTIDV is the amino-terminal end of the extended helical region of *Drosophila* moesin; see Fig. 3 of Edwards *et al.*, 1994).

Transformation and induction of hs-GFP-moe. Several transgenic lines bearing different insertions of this construct were obtained by injecting DNA into *w*;Δ*2-3* embryos by standard methods (Robertson *et al.*, 1988; Ashburner, 1989), except that eggs were not dechorionated, but cleared with halocarbon oil prior to injection. We obtained nine transformed progeny from 33 surviving embryos injected with DNA purified using Wizard Maxipreps (Promega, Madison, WI). Transcription of *hs-GFP-moe* was induced by placing glass culture vials (9.5 × 2.5 cm, weight 28 g including fly agar–yeast food medium) in a 37°C room for 50 min. Occasionally a double heat shock was used for stronger induction (50–60 min, 37°C; 60 min, 21 to 25°C; 50–60 min, 37°C). Most transformed lines express GFP in response to heat shock, though the amount of protein produced varied between lines presumably due to position effects. Fluorescence was not easily visible until 2–4 hr after induction. Two inserts on the second chromosome that produce strong fluorescence were recombined to yield a two-copy chromosome, maintained over a balancer (*hs-GFP-moe 2.3, 2.6/SM6a*). Animals homozygous for this chromosome are fertile, but show reduced viability due to one of the insertion sites. As a consequence we keep them both as a semibalanced stock and a homozygous stock. Since no specific phenotypic difference was noted between the heterozygous two-copy and homozygous four-copy animals, they were used interchangeably for most experiments.

Microscopy. Ovaries and pupal tissues were dissected in EBR (Montell *et al.*, 1992) and either fixed in fresh 2% paraformaldehyde in PBS for 10 min or mounted in Schneider's tissue culture medium (Schneider and Blumenthal, 1978) and viewed live. For longer term observation (>1 hr), the drop of medium was prevented from spreading by a circle of vacuum grease painted on the slide, and the coverslip was supported by a picture frame-shaped piece of dry filter paper, with an air-filled gap between the medium and the paper to provide some oxygen to the sample (Lutz and Inoué, 1986). For long-term observation of embryos, eggs were dechorionated by standard methods, immersed in a 1:1 mixture of halocarbon 27 and 700 (Halocarbon Products Corp., N. Augusta, SC), and then mounted in a Teflon windowed chamber that allows observation at high resolution (Kiehart *et al.*, 1994). Actin staining was performed as described (Edwards and Kiehart, 1996). Samples were viewed with a Zeiss LSM 410 or Bio-Rad MRC600 confocal scanning head microscope attached to a Zeiss Axioskop stand equipped with Zeiss optics. Images were collected with the following Zeiss lenses: 25× multi-immersion 0.8 NA; 40× multi-immersion 0.9 NA; 40× water immersion 1.2 NA; and 63× oil immersion 1.4 NA. For double-labeling the following excitation/emission wavelengths (nm) were used: GFP, 488/ 515–540; rhodamine, 568/>590; chorion autofluorescence, 488, 568, and 647 simultaneously/>590. Scanning confocal time-lapse series were collected with the Bio-Rad scanning head microscope and Zeiss Axioskop system using a GFP filter set made by Bio-Rad.

Nomenclature. *Drosophila* moesin, the product of the *Moesin-like* (*Moe*) gene, was previously referred to as D17 or MER-like protein by Edwards *et al.* (1994) and called Dmoesin by McCartney and Fehon (1996). In Flybase (Internet address http://cbbridges.harvard.edu:7081), D17, Emr1, and Ezrin-moesin-radixin-1 are listed as acceptable synonyms. While nominally more similar to moesin than radixin or ezrin, fly appears to have only one of the three, so it may well be that the fly protein could be considered orthologous to all three of its vertebrate cousins. The GFP-moesin tail fusion protein described here is abbreviated as GFP-moe, and the transgene that encodes it is referred to as *hs-GFP-moe*.

Moesin antisera. A pGEX-moesin tail bacterial expression construct was generated. The moesin tail coding region was PCR amplified using primers D17-BamCla-f (5′-ccgggatccatcgatgtgcagcagatg) and D17-CtRI-r (5′-ctctcgaattcccgcgcactatcgatc), digested with *Bam*HI and *Eco*RI, and subcloned into *Bam*HI/*Eco*RI-digested pGEX-2T (Pharmacia, Piscataway, NJ). High levels of soluble GST-moesin fusion protein were recovered and used to immunize rabbits, yielding two polyclonal sera (DU3 and DU4) that specifically

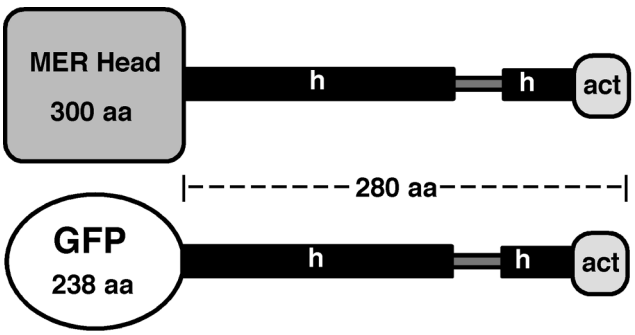

FIG. 1. Schematic representations of moesin and GFP-moe. Top, intact moesin; bottom, the fusion protein used in this study. ''MER Head'' domain is highly conserved among all moesin/ezrin/radixin family members. Thick black bars indicate extended helical regions that structure prediction algorithms suggest participate in the formation of coiled coils (''h''; Lupas *et al.,* 1991; Berger *et al.,* 1995). ''act'' indicates the actin binding site (Turunen *et al.,* 1994). Approximate sizes are given in amino acids.

TABLE 1
Summary of *hs-GFP-Moe* Expression and Localization

Location	Characteristics
All somatic tissues	Outlines cells, concentrates in cell surface projections
Ovary	Follicle cell specific—not expressed in germ cells
Polar follicle cells	Specific labeling persists for 3 days
Border cell process	Interacts with microtubules?
Embryos	Earliest expression using *hsp70* system: Elongated germ band stage; highlights denticle belts
Neurons	Concentrates due to axonal actin or tubulin?
Eye imaginal disc	Concentrates in center of each ommatidium; highlights morphogenetic furrow
Muscle	Poor expression in IFM, but sarcomeric pattern can be seen in leg muscle

recognize the GST-moesin fusion protein and a single species of appropriate M_r from whole flies. Western blots were probed with DU3, which was detected using the ECL system (Amersham, Arlington Heights, IL). Western blots were analyzed by scanning the films and quantifying each band using NIH Image software. Multiple different exposures were analyzed and nonlinear response of the scanner was corrected using density standards; however, linear response of the ECL system to increasing protein concentration was not tested.

RESULTS

The *Drosophila* moesin tail was tagged with GFP to track its cellular distribution in living flies. We define the moesin tail as the C-terminal portion of the protein following Pro43 and refer to it as moe (Pro296 in full-length human moesin; see alignment and references in Edwards *et al.,* 1994). According to secondary structure predictions, this Pro is followed by an extended α helix shared by all reported members of the ezrin/moesin/radixin family (Fig. 1). The α helical region is followed by a conserved actin binding site at the very C-terminus (Turunen *et al.,* 1994). We fused the wild-type GFP cDNA to the moesin tail coding region so that GFP replaces the slightly larger moesin head domain (Fig. 1). The fused coding region was placed under control of the *hsp70* promoter in a *P* transposable element vector to yield *hs-GFP-moe*. A transformed line bearing two independent insertions of this construct (*hs-GFP-moe 2.3, 2.6/SM6a*) was used for the following experiments (see Materials and Methods). Following heat shock induction of the transgene, a fluorescent signal appears in most tissues of embryos, larvae, pupae, and adults (detailed below and summarized in Table 1). The GFP signal is comparable in strength to the signals we typically observe with immunofluorescence and rhodamine–phalloidin labeling of fixed tissues (Edwards and Kiehart, 1996). (Our transformants were made prior to the introduction of improved mutant GFPs that would presumably yield an even brighter signal.)

Western analysis of hs-GFP-moe expression. To determine if the GFP signal originates from intact GFP-moe, we examined the expressed protein by Western blotting (Fig. 2). Extracts of adult females (*hs-GFP-moe 2.3, 2.6/SM6a*) were prepared at various times after heat shock, blotted following SDS–PAGE, and incubated with DU3 polyclonal serum. DU3 was raised against exactly the same portion of moesin that is expressed by *hs-GFP-moe;* therefore, this serum should detect the endogenous moesin and GFP-moe equally well. In uninduced and wild-type flies, a single band is found in the position expected for full-length moesin (~68 kDa). A single band of ~60 kDa, the predicted size of GFP-moe, appears 1.5 hr after a 1-hr heat shock. This protein accumulates to a level ~30–50% as great as the level of endogenous moesin, as determined by densitometry of

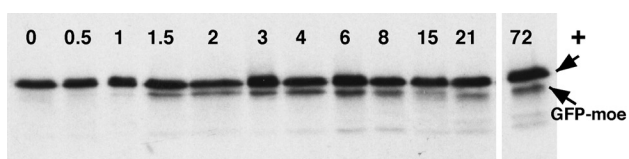

FIG. 2. Western analysis of heat shock-induced GFP-moe expression in whole flies. Females bearing two copies of the *hs-GFP-moe* transgene were given a 1-hr heat shock and later homogenized. Extracts were separated by SDS–PAGE and probed with moesin tail antiserum. Time (hr) between the end of the heat shock period and the homogenization is given above each lane. The upper band (+) corresponds to endogenous, full-length moesin also seen in wild-type flies. The lower, inducible band has the mobility expected for GFP-moe.

the Western blot signal. GFP-moe is still readily detectable 3 days after heat shock, even though protein in the follicle cells is eliminated as the oocytes mature. Together with the following experiments, this result shows that the fusion protein is highly stable *in vivo.*

Effects of hs-GFP-moe expression. *hs-GFP-moe 2.3, 2.6* flies remain normal and fertile even when maintained on a daily heat shock regimen for multiple generations, demonstrating that the fusion protein does not overtly disrupt development. However, we do note two transient effects of fusion protein expression. First, after about 20 min at 37°C, the transgenic flies become paralyzed. In marked contrast, their siblings without the transgene remain extremely active. The paralyzed flies recover quickly and are not obviously harmed. Second, in the first few hours after heat shock, GFP concentrates in fine cell surface projections (filopodia or microvilli) that appear on oocyte follicle cells (see below), border cells, and other cell types (not shown). In certain cases, these projections are absent the next day, even though the fusion protein is still present (e.g., the border cells of the oocyte; see below).

GFP-moe localization in embryos. We heat shocked and observed both *hs-GFP-moe* and control embryos by confocal microscopy. The GFP signal is easily detectable in intact eggs that have had their chorions cleared by halocarbon oil, though we typically dechorionate the eggs for clarity. With proper oxygenation and an intact vitelline membrane, the embryos will complete development and hatch while under observation in halocarbon oil. In control embryos that do not express GFP (e.g., wild-type embryos or embryos that carry the *hs-GFP-moe* transgene but have not been heat shocked), no cellular fluorescence is seen even under high gain, although there is autofluorescence associated with the yolk (Fig. 3A). In *hs-GFP-moe* embryos, epidermal cells are outlined by a strong, specific GFP signal at the cell cortex (Fig. 3B). This cortical labeling highlights the arrangement and shape of various cell types (Figs. 4A and 4B). During dorsal closure, the actin-rich leading edge of the migrating lateral epidermis is strongly labeled (Figs. 4C and 5; see below and Young *et al.*, 1993). Segmental landmarks are clearly visible, including forming tracheal pits (not shown) and sensory structures such as the chordotonal organs (Fig. 6A). Denticles accumulate the fusion protein even before they form cuticle, making it a potential, early marker for segmental patterning (Fig. 4D). The developing central nervous system is intensely labeled by the fusion protein, perhaps because it is also actin-rich (Fig. 6B). Even embryos that are just about to hatch are strongly labeled (Fig. 6C). In contrast, immunofluorescence is difficult to perform at this stage due to problems with antibody penetration.

GFP-moe allows dorsal closure to be imaged in living specimens. At appropriate stages, the cellular events that underlie gross morphological rearrangements in the embryo can be imaged. In the later embryo, this includes germ band retraction, dorsal closure, head involution, and gut morphogenesis. The utility of this construct in dorsal closure is particularly instructive. The lateral epidermis on either flank of the embryo spreads dorsally to meet at the dorsal midline (Young *et al.*, 1993; Fig. 3.4 in Campos-Ortega and Hartenstein, 1985; Hartenstein, 1993). At their leading edge the dorsal-most cells of the lateral epidermis are very thin, and attempts to image the leading edge with differential interference microscopy have proven extremely difficult and cannot be done reliably, largely because of the refractile yolk and gut structures that lie just beneath the epidermis and the amnioserosa. In contrast, GFP-moe binds to the actin-rich purse string at the leading edge and allows us to follow dorsal closure easily (Figs. 4C and 5; see also the QuickTime movie of this process at http://note.cellbio.duke.edu/Faculty/~Kiehart/). The images confirm that the leading edge proceeds dorsally in a smooth front, consistent with the purse string hypothesis that we proposed earlier (Young *et al.*, 1993).

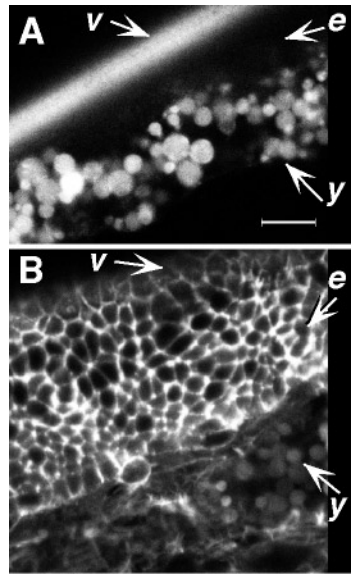

FIG. 3. Confocal optical sections show the specificity of the GFP signal. Two embryos were heat shocked identically, dechorionated, mounted in halocarbon oil, and viewed live at extended germ band stage. (A) Negative control embryo carrying a CaSpeR-hs *P* element vector with a non-GFP insert (*P*[*hs-sqh*$^+$]; Edwards and Kiehart, 1996). At high gain, the vitelline membrane (*v*) and yolk (*y*) are autofluorescent, but no signal is detectable in epidermal (*e*) or other cells. (B) Embryo carrying a CaSpeR-hs *P* element vector with the *GFP-moe* insert (two or four copies). At medium gain, the GFP signal outlines cells and is detectable well over the background of the yolk and vitelline. Bar, 10 μm.

Localization in larvae. The lining of the gut accumulates a high concentration of GFP-moe (not shown). EM studies show that the *Drosophila* gut is lined with brush border microvilli that are ultrastructurally similar to the actin- and ezrin-rich microvilli of vertebrate intestinal cells (Morgan *et al.*, 1995). The fusion protein probably accumulates in these microvilli, though we cannot resolve them by light microscopy.

The developing eye imaginal disc also produces actin-rich microvilli, notably at the apices of cells in the morphogene-

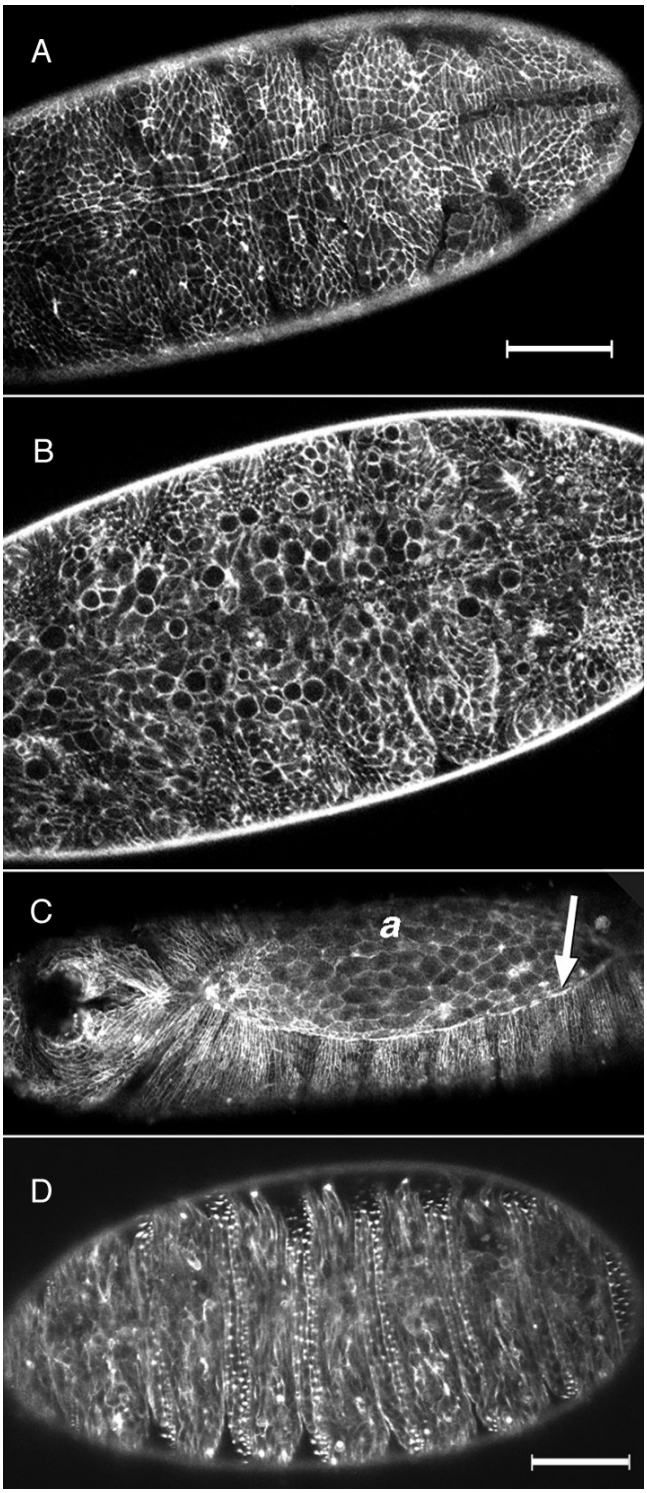

FIG. 4. GFP-moe distribution following induction in embryos. Confocal optical sections of live embryos carrying two or four copies of *hs-GFP-moe*, ~3 hr after a double heat shock. (A) Ventral surface of an extended germ band embryo. Apical domains of epidermal cells are outlined. Bar, 50 μm for all panels. (B) More medial section of the embryo in A shows cell outlines in the epidermis, mesoderm, and neuroblasts. (C) Section through the dorsal surface of an embryo during dorsal closure. The actin-rich leading edge of the lateral epidermis is highlighted (arrow). (D) Surface view of an embryo shows GFP-moe in the actin-rich denticles.

tic furrow and the rhabdomeres of photoreceptor cells (Wolff and Ready, 1993). These structures appear to accumulate the fusion protein as well, as indicated by the specific labeling of the furrow (not shown) and the center of each ommatidial cluster after the furrow passes (shown in pupal specimens, below).

Localization in pupae. Fine details of the developing pupal CNS and visual system are vividly highlighted by the GFP-moe (Fig. 7). In addition to the rhabdomeres and/or cell bodies of the photoreceptors, axons are labeled as they project in an ordered fashion into the lamina and then to the optic lobes (Figs. 7a and 7b). Thoracic and abdominal neuromeres are apparent (Fig. 7b). In the retina, the arrangement of ommatidia and their constituent cells can be seen (Fig. 8a). The presumptive margin of the wing is revealed by a double row of bristle precursors (Fig. 8b). In later stage female pupae, the somatic cells of the ovary, especially the terminal filaments, are prominent (Fig. 9a). Some muscles show a striated GFP signal, though it is weaker and more variable than one might expect given the quantity of actin present (not shown). The indirect flight muscles that pack the thorax accumulate very little fusion protein and no striations are evident. We suspect that the moesin binding site on actin is occluded to a greater or lesser extent in different muscle types.

Localization during oogenesis. The fusion protein uniformly outlines the somatic follicle cells as they encase individual germ cell cysts in the germarium and subsequently form egg chambers separated by interfollicular stalks (Fig. 9b; see Spradling, 1993, for review of oogenesis). GFP signal is most intense at the apical (inner) ends of the follicle cells, but the signal is not polarized in the interfollicular stalk cells. Germ cells are relatively devoid of signal, apparently because the heat shock promoter is, in this case, not strongly inducible in the germline (Fig. 9b). With high gain, a faint signal is detectable at the nurse cell membranes and the ring canals, the actin-rich structures lining the passages between the germ cells (not shown; Mahajan-Miklos and Cooley, 1994).

In stage 10 egg chambers, most follicle cells belong to two populations: the oocyte follicle cells, which form a columnar epithelium over the oocyte, and the nurse cell follicle cells, which flatten and spread over the adjoining nurse cells. From the basal (outer) ends of the oocyte follicle cells protrude extremely long microvilli that exhibit bright fluorescence (Fig. 10A). Comparable projections cannot be seen by phalloidin staining in wild-type chambers, suggesting that they may actually be induced by expression of the fusion protein. The apical ends also show microvilli (Fig. 10C), but they are much shorter than the basal projections and indistinguishable from microvilli seen in wild-type phalloidin-stained chambers. GFP signal is not seen at the lateral

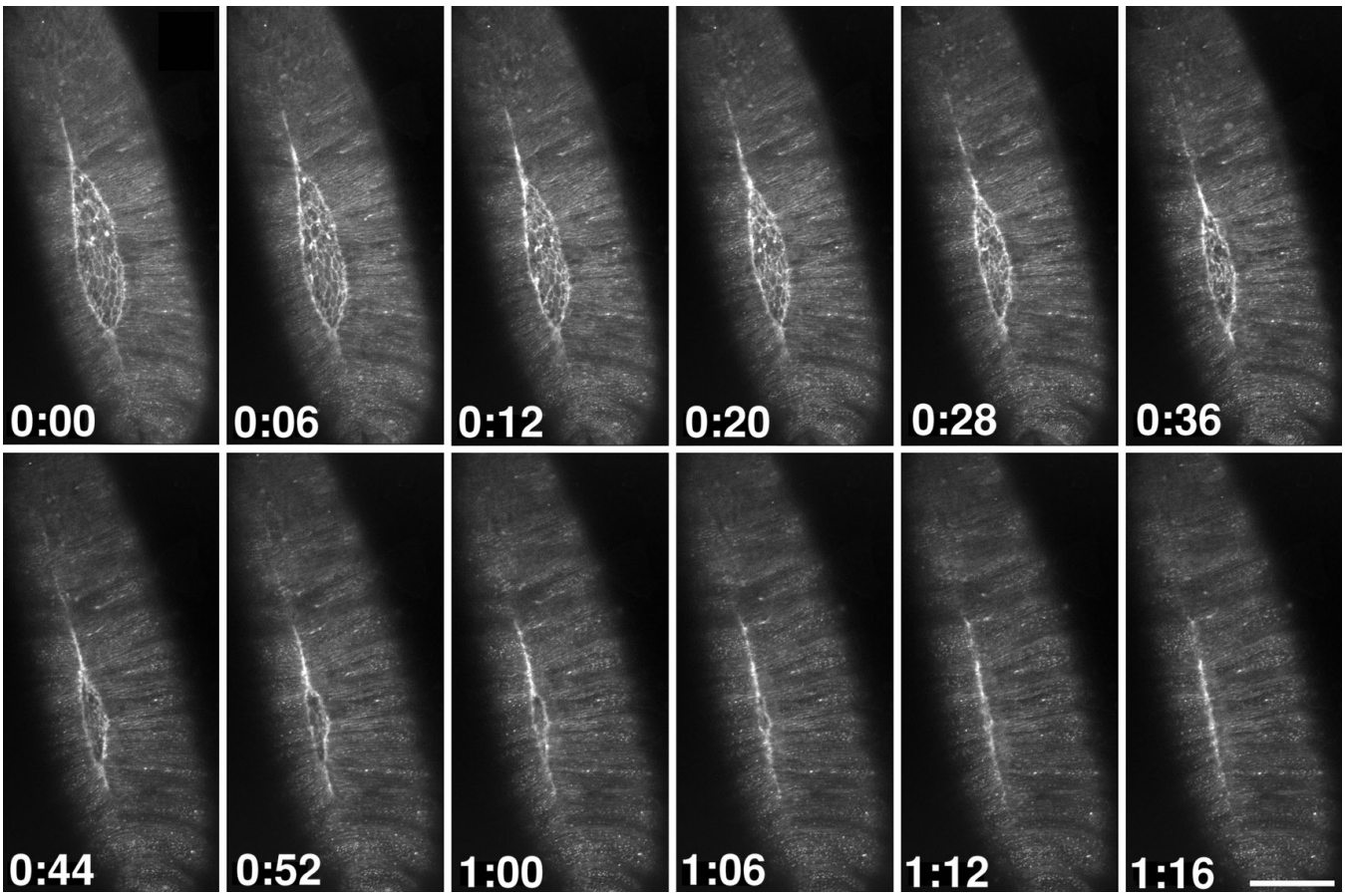

FIG. 5. Dynamics of dorsal closure. Selected images from a low-resolution, time-lapse confocal sequence of dorsal closure in a double heat shocked embryo (originally images were taken once every 3 min). GFP-moe shows cell sheet spreading during dorsal closure. Time is shown in hours:minutes from the time that the first image was collected. Scale bar is 100 μm. See also the QuickTime movie of dorsal closure at http://note.cellbio.duke.edu/Faculty/~Kiehart/.

membranes (Fig. 10B). In contrast to the oocyte follicle cells, projections are not visible on the nurse cell follicle cells, and on earlier stage follicle cells only short, sparse projections appear (not shown).

Tracking polar follicle cell behavior. A pair of cells at each end of the newly formed egg chamber, called polar follicle cells (PFCs), are specified to differentiate from the rest of the follicular epithelium. The PFCs express characteristic marker proteins, adopt specific morphologies, and cease proliferation (Spradling, 1993; Margolis and Spradling, 1995). This last property allows us to specifically label these cells by transiently inducing *hs-GFP-moe* (see above). One day after induction, the GFP signal in the PFCs remains strong as the signal in the other follicle cells is diluted by proliferation (Fig. 9b). Two days after induction, the PFCs are labeled with high specificity (Fig. 11). Stalk cells also stop dividing and remain labeled (Fig. 11a).

While most follicle cells move posteriorly over the growing oocyte, approximately eight cells (border cells) at the anterior tip of the egg chamber delaminate from the follicular epithelium (Montell *et al.*, 1992). They migrate between the nurse cells toward the anterior face of the oocyte, remaining tightly adherent to each other as they crawl. After arriving at the oocyte, they are met by centripetally migrating follicle cells and collaborate with them to form the micropyle, the sperm entry port in the mature eggshell (Montell *et al.*, 1992). We find that the anterior PFCs, observed using GFP-moe, are invariably included in the border cell cluster. In fact, the PFCs are always found in the same position, central in the cluster (Figs. 11b–11d). This suggests that they have a key role in organizing the border cells.

The PFCs play another important role after the border cells arrive at the oocyte. The PFC touches the oocyte with a broad cell surface projection (Fig. 11d). As the micropyle is built, the projection extends and narrows to form the border cell process (Fig. 11e). This process penetrates the micropyle, creating the central canal through which the sperm enters (Zarani and Margaritis, 1986; Montell *et al.*, 1992). At all stages this projection is labeled even more

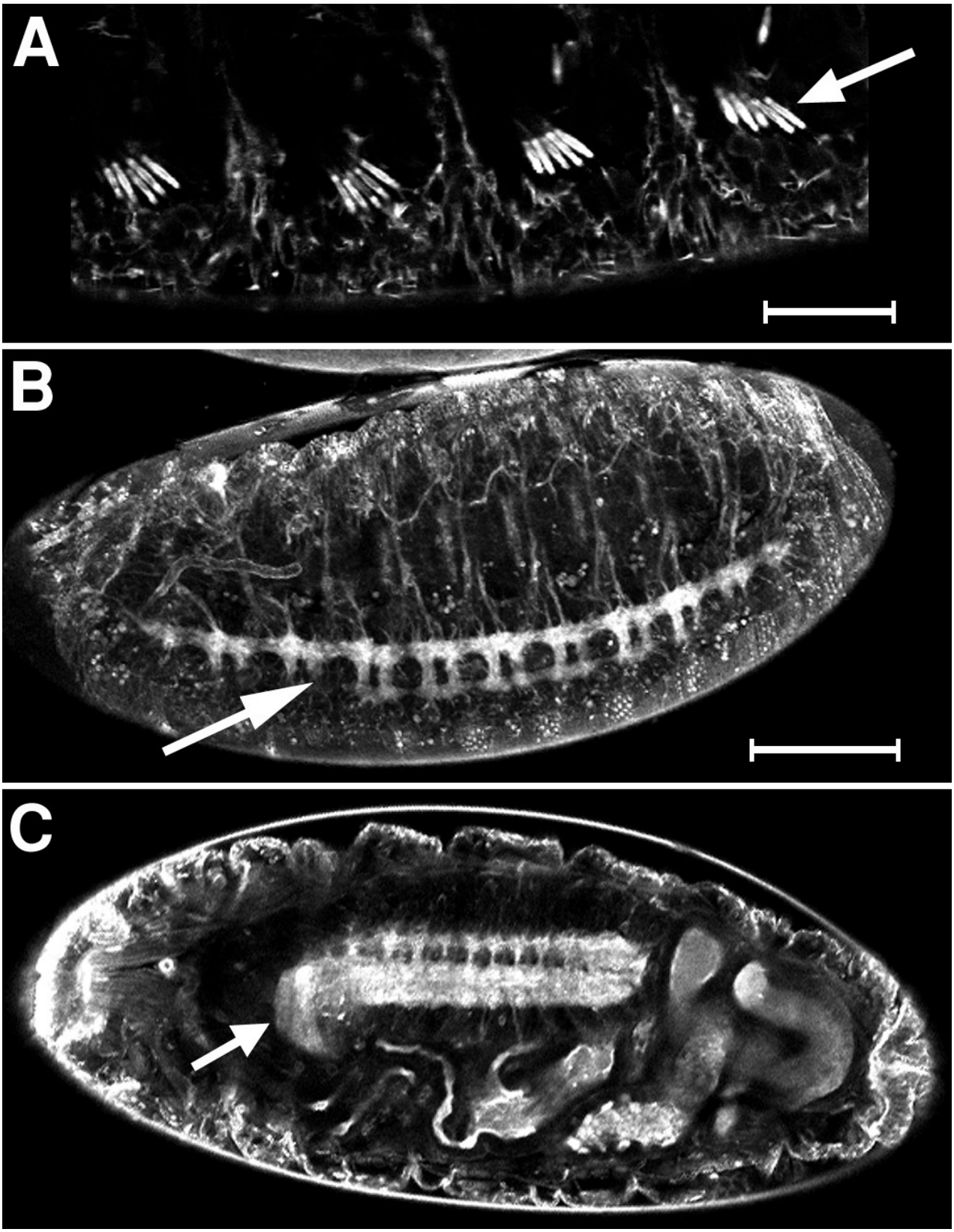

FIG. 6. Nervous system development can be examined using GFP-moe. Embryos are as described in the legend to Fig. 4. (A) A portion of the chordotonal organ is brightly labeled (a bundle of five chordotonal organs occur in each segment, arrow). Bar, 40 μm. (B) Condensing CNS (arrow) is brightly fluorescent in a midstage embryo (projection of confocal Z series). Bar for B and C, 80 μm. (C) Late stage embryo: brain (arrow), attached ventral ganglion, and gut are highlighted as the embryo moves vigorously within the vitelline membrane.

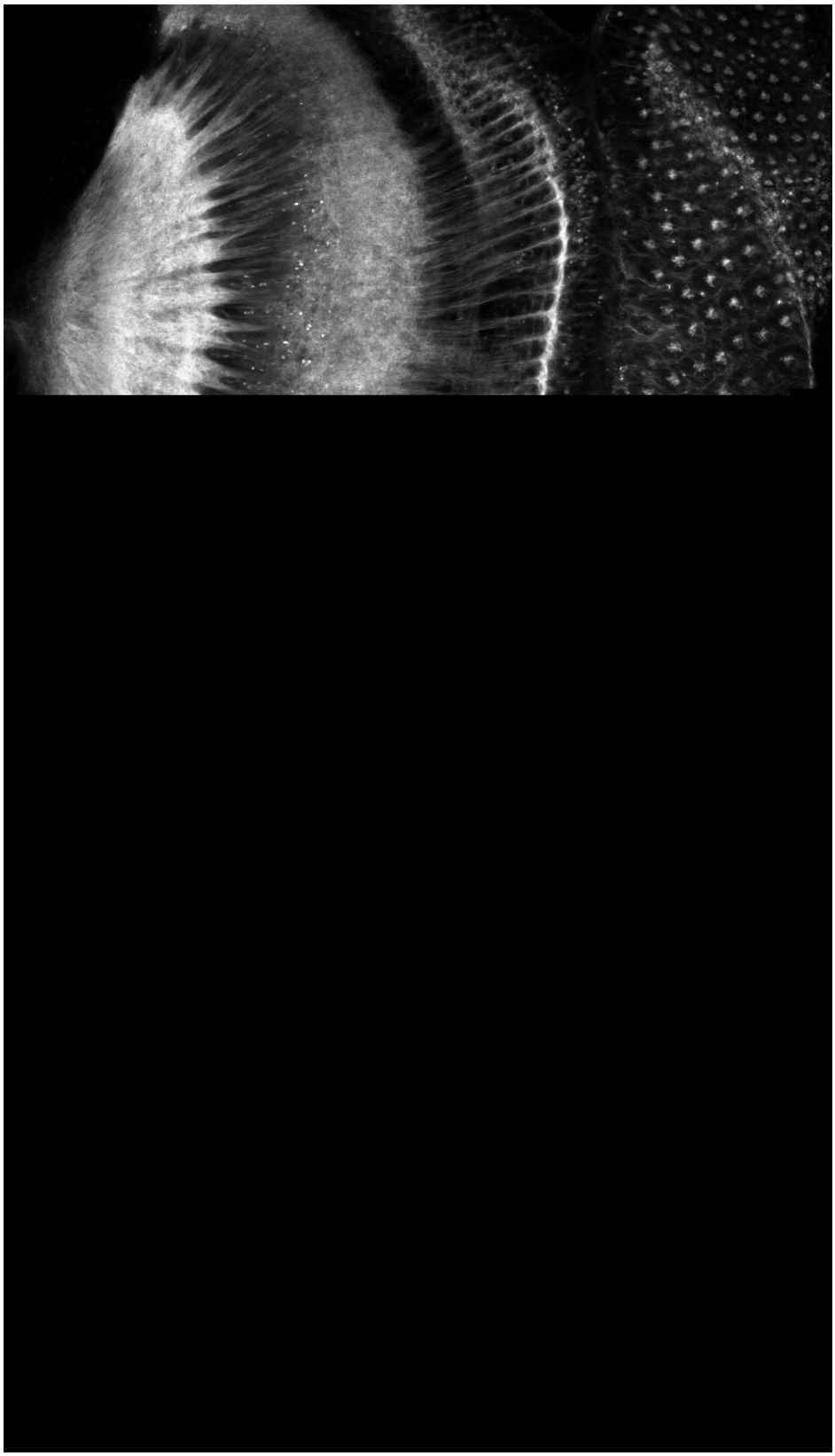

FIG. 7. Confocal optical sections of a live CNS and visual system cultured from a pupa carrying four copies of *hs-GFP-moe*, dissected 29 hr (after pupa formation) at 24°C, following 40-min heat shocks at 17 and 20 hr APF. (a) Axons project from the retina (*r*) into the developing optic lobe. (b) Intact CNS: retina is seen in each upper corner peripheral to the optic lobes (*ol*). Brain (*b*), thoracic (*t*), and abdominal ganglia are located centrally in the panel.

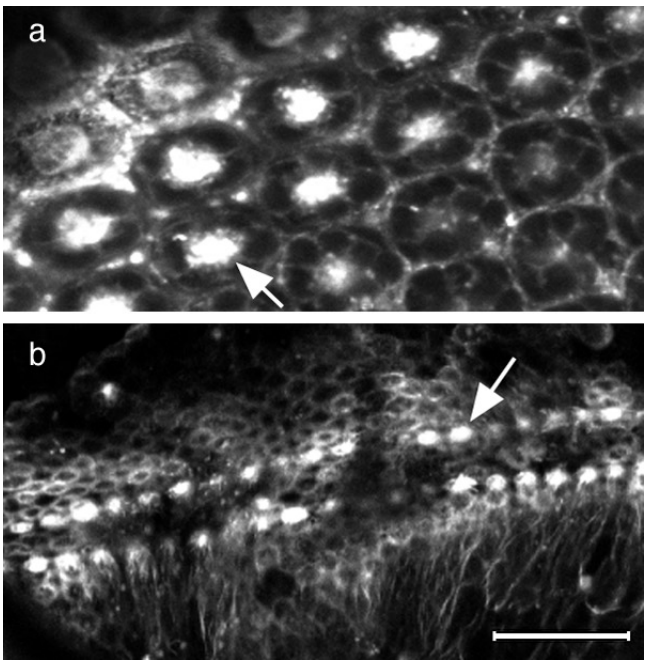

FIG. 8. Localization patterns in pupal wing and retina. Samples prepared as in Fig. 6. (a) Eye imaginal disc, 48 hr APF. Ommatidial clusters are seen at various focal planes as the disc curves away (outer surface of the retina is seen at the upper left). Photoreceptor cells show extremely high GFP signal (arrow). (b) At 29 hr APF, the presumptive margin of the wing imaginal disc is revealed by a double row of cells (most likely bristle precursors) that strongly accumulate the fusion protein (arrow). Bar, 20 μm for both.

intensely than the cell body. Our observations suggest that the anterior PFCs are fated early in oogenesis to eventually form the micropylar canal. Since there are many cells in the region secreting autofluorescent chorion material, this provides a unique and powerful method for following this important developmental process in living specimens. Our results with live specimens agree strongly with such published accounts of micropyle formation (Zarani and Margaritis, 1986), suggesting that the fusion protein does not interfere with cell behavior. Interestingly, Zarani and Margaritis show that the border cell process is rich in microtubules, suggesting that its morphogenesis may be dependent on both actin- and microtubule-dependent processes.

DISCUSSION

A wealth of information has been gained by using cell type-specific markers (for example, enhancer traps) to examine mutations that disrupt cell fate specification. In a similar fashion, GFP marker proteins that label subcellular compartments can greatly enhance the analysis of mutations that disrupt differentiation and morphogenesis. Here we describe a new tool of this class that can be used to examine dynamic processes such as actin reorganization, cell shape change, and cell migration in intact animals. Though it is based on a *Drosophila* protein, this tool can be used in a variety of organisms.

Transgenic flies were produced that express a chimeric protein consisting of GFP fused to the C-terminal half of the *Drosophila* moesin homolog. Both halves of the chimera retain their normal *in vivo* functions: the GFP portion yields bright fluorescence in living cells, while the moesin tail associates with the actin-rich cell cortex and cell surface projections. The moesin tail has two domains that can account for this localization pattern. First, at the C-terminus lies an actin binding site that is especially active in the absence of the N-terminal MER head (Fig. 1; Turunen *et al.*, 1994; Gary and Bretscher, 1995). This C-terminal domain presumably allows fusion protein to bind actin even where endogenous moesin is absent. This would explain how GFP-moe could bind to the I band in striated muscle where there is no endogenous moesin. The C-terminal domain may also bind endogenous moesin, as suggested by Gary and Bretscher (1995) for mammalian ezrin. Second, through protein sequence analysis with coiled coil prediction algorithms (Lupas *et al.*, 1991; Berger *et al.*, 1995), we identified a heptad repeat in the region previously predicted to form only an extended alpha helix. That this region may mediate the formation of a coiled coil structure was previously missed. Such a structure may play a role in the known dimerization and oligomerization of MER proteins observed when the MER proteins are isolated from cells (Gary and Bretscher, 1995, see also Oas and Endow, 1994, for a discussion of the dynamic nature of coiled coils). This domain could allow the fusion protein to ''piggyback'' onto endogenous moesin as it assembles into cell surface projections. The precise role of this region in MER protein function will have to await more thorough biochemical characterization of its behavior in solution.

Phenotypic effects of GFP-moe expression. The GFP-moe coding region was placed under control of the *hsp70* promoter so that high-level expression of the fusion protein could be induced by heat shock. Western analysis shows that flies with two copies of the transgene express the fusion protein within 90 min after heat shock, although fluorescence is not easily detectable for another 1–2 hr. The fusion protein persists intact for at least 3 days and remains localized near the cell surface, suggesting that the protein becomes stably integrated into the membrane cytoskeleton.

The onset of expression has two surprising effects. Upon induction, flies expressing the fusion protein become paralyzed, but they soon recover and appear to behave normally. Since the fusion protein concentrates in neuronal processes and might induce changes in cell morphology (see below), we suspect that the moesin tail causes a temporary mechanical disruption of motor neuron synapses or other neuronal structures upon its first appearance. Since the fusion protein persists for days, but the paralysis lasts for 5 to 10 min, it appears that the fly can quickly adapt to the presence of the moesin tail.

Second, long membrane processes appear on specific cell

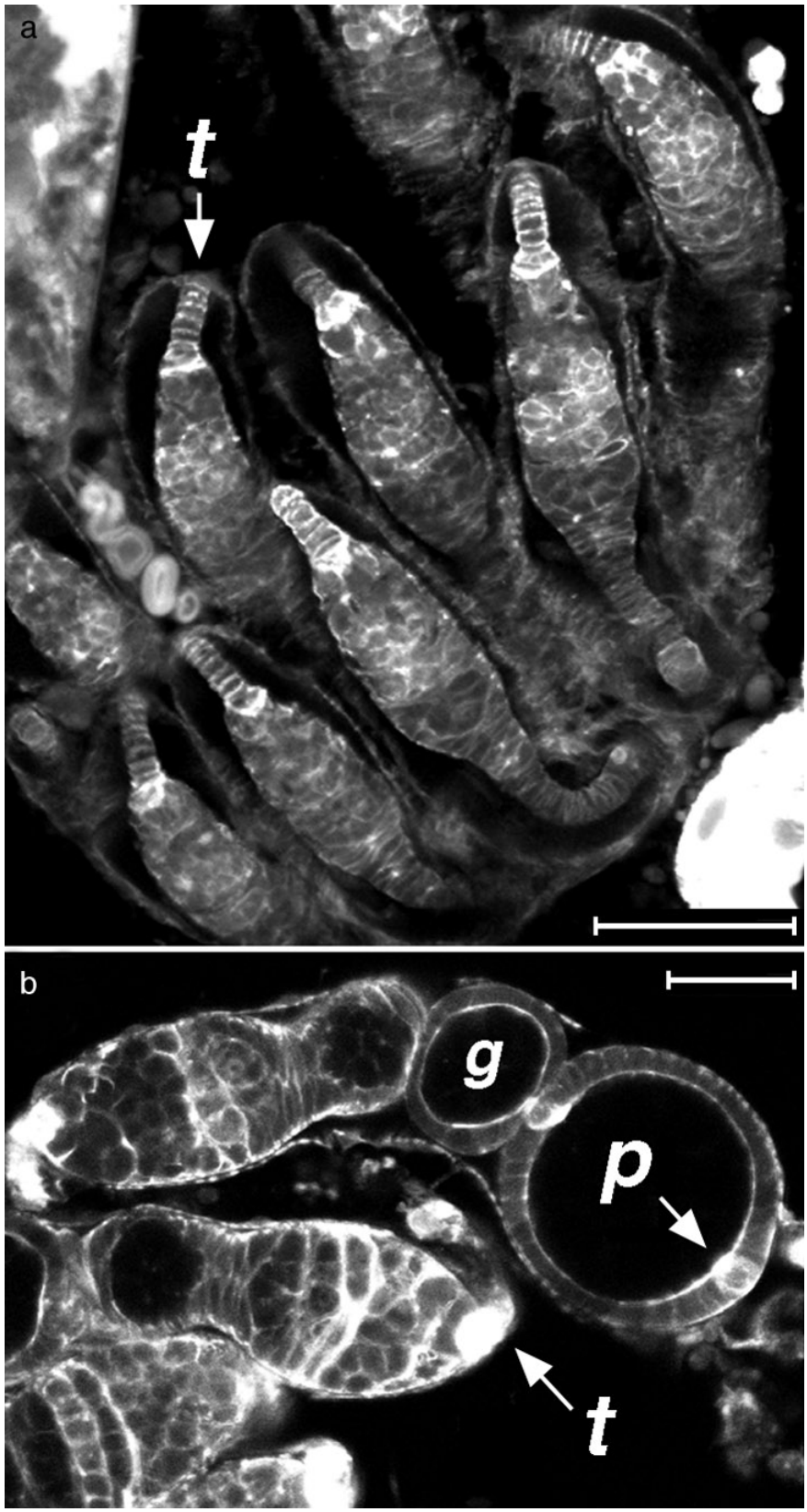

FIG. 9. Localization in developing ovarioles. (a) Developing ovary in a later stage female pupa, fixed ~3 hr after induction of GFP-moe. Bar, 50 μm. (b) Live germaria and early stage egg chambers from an adult ovary, 24 hr after induction of GFP-moe. The somatic cells of the ovary are prominent, though the germ cells (*g*) appear dark since they express little GFP. In the polar cells (*p*) and terminal filaments (*t*), signal is especially strong since the protein is not diluted by cell proliferation. Bar, 25 μm.

surfaces within 2 hr after induction of the protein. In most cases it is unclear whether the fusion protein stimulates new processes, elongates preexisting processes, or simply accumulates in normal processes that are difficult to see by other means. However, the GFP-moe used here can stimulate filopodia to form when expressed in COS cells (Edwards. K. A., Kiehart, D. P., and Alcorta, D. A., unpublished observations). Henry *et al.* (1995) similarly found that the radixin tail can promote filopodia when overexpressed in NIH-3T3 cells. Moesin family proteins seem to be intimately involved in the regulated assembly of cell surface projections, and the moesin tail fragment appears to be capable of deregulating some aspect of this process. Using GFP-tagged moesin fragments such as the one described here, it should be possible to directly observe the effects of various domains of the protein on the behavior of dynamic membrane structures in live cells.

Importantly, animals with at least two to four active copies of *hs-GFP-moe* can be maintained over several generations on a daily heat shock regimen of 50 min at 37°C. Despite the continuous presence of the fusion protein, we find no external morphological defects, and the flies remain

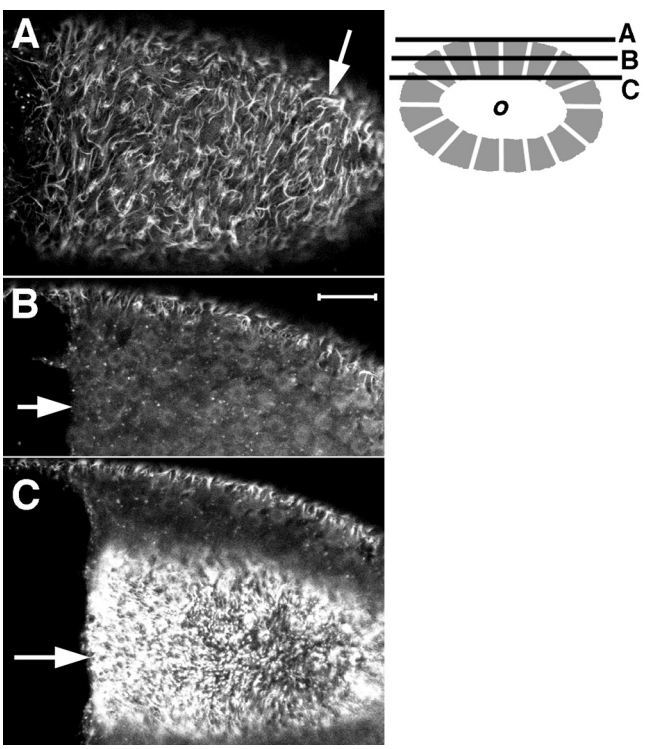

FIG. 10. Microvilli are labeled by GFP-moe in a live stage 10 *hs-GFP-moe* egg chamber ~4 hr after induction. Schematic diagram shows a cross-section of the egg chamber (A–P axis projecting from the page), with the columnar oocyte follicle cells (gray) covering the oocyte (*o*). The focal planes of each optical section are indicated by black lines. (A) Long cell surface projections are evident on the basal (outer) surface of the follicle cells (arrow). (B) Slightly deeper focal plane of the same chamber; nuclei are faintly visible (arrow) but the lateral follicle cell membranes are devoid of fusion protein. (C) Apical microvilli (arrow) of the same follicle cells appear shorter but brighter than the basal projections in A.

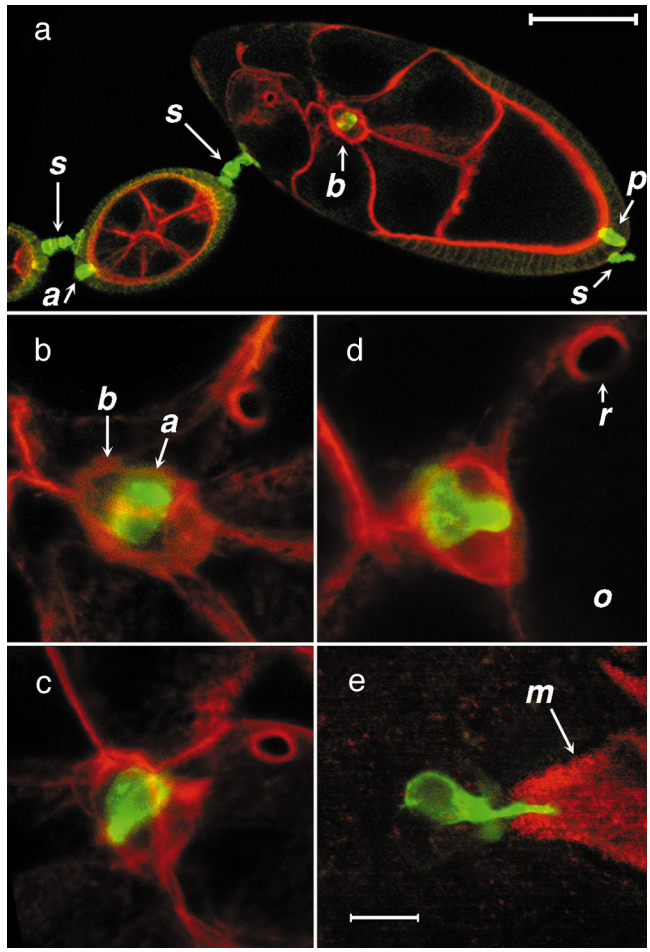

FIG. 11. Tracking polar follicle cell development with GFP-moe. Egg chambers from *hs-GFP-moe* females (1–2 days after eclosion, 2 days after last heat shock induction of *hs-GFP-moe*) were examined by confocal microscopy; green indicates GFP signal. Anterior is left. (a–d) Egg chambers fixed and stained with rhodamine–phalloidin (shown in red) to highlight cell outlines and ring canals (*r*). (A) GFP-moe protein specifically labels the interfollicular stalks (*s*) and polar follicle cells (PFCs). The anterior PFCs (*a*) become incorporated into the migrating border cell cluster (*b*) at stage 9, while the posterior PFCs (*p*) remain in the follicle cell layer. Bar, 50 μm. (b, c) Close-ups of migrating border cell clusters. The PFC always occupies a central position in the cluster and typically shows an asymmetric distribution of GFP-moe, such as the lateral bulge in (c). b is from the chamber shown in a. (d) Stage 10 border cell cluster has completed migration and abuts the oocyte (*o*). The PFC remains in the center of the cluster and adopts a characteristic pear shape at this stage, with the narrow end touching the oocyte and displaying a high concentration of fusion protein. (e) Live, cultured egg chamber (no phalloidin). Autofluorescence of the chorion material that forms the micropyle (*m*) is shown in red. The PFC extends a long process into the central bore of the micropyle. (b–e) Same scale: bar, 10 μm.

fertile. Even structures that are sensitive to disruption, such as bristles and rows of ommatidia, remain normal. Overall viability may be reduced, but this can be attributed to the effects of heat shock alone. While the transgene has little effect on wild-type flies, it should still be considered a candidate for interaction with various cytoskeletal and signaling mutations. However, since *hs-GFP-moe* is well-tolerated by the fly, we believe it can be treated as a relatively nondisruptive *in vivo* marker for most applications.

A stable marker for specific cells. While the heat shock promoter is typically used to drive ubiquitous expression of transgenes, in this study we find two fortuitous effects that allow labeling of specific cells. First, the promoter is expressed very weakly in the germline. This effect may be construct-specific, since we have used the same promoter/vector combination for expression of nonmuscle myosin regulatory light chain in the germline (Edwards and Kiehart, 1996). Since the nurse cells provide no background signal, we can clearly observe several follicle cell populations that migrate over and through these germ cells during egg morphogenesis. This should permit time-lapse video analysis of these migrations in wild-type and various mutant backgrounds, once methods for the long-term culture of egg chambers are devised.

The fusion protein is transiently expressed after heat shock, but has a long half-life in the cell. When a proliferating epithelium is heat shocked early in its development, all cells are initially labeled, but the signal grows dim as the GFP-moe is diluted by cell division. However, the fusion protein persists undiluted in any nondividing cells in the tissue, and therefore these cells become specifically labeled. In addition, cell type-specific differences in the cytoskeleton as well as other factors may contribute to the perdurance of specific labeling. This phenomenon is apparent during both oogenesis (Fig. 11) and imaginal disc development. For example, in egg chambers the polar follicle cells remain strongly labeled after several days, and in the leg disc only a handful of cells (apparently corresponding to the *neuralized*-expressing sensory organ precursors) remain brightly fluorescent 2 days after heat shock (not shown).

Uses for GFP-moe. To identify potential uses of the fusion protein, we have examined its distribution in animals at various developmental stages by scanning confocal microscopy. The fluorescent pattern we observe is very similar to the pattern produced by staining actin with fluorescent phalloidin. The GFP signal, however, is more strongly concentrated in cell surface projections (Fig. 10A) and near the plasma membrane than phalloidin, with little signal detected in the cytoplasm (Fig. 3B). Also, the GFP signal in live tissue is not subject to problems of stain penetration or other fixation artifacts. Therefore, the fusion protein offers an improved method for analysis of cell sheet morphogenesis. Rather than comparing fixed, phalloidin-stained tissues from a range of stages, changes in cell shape and pattern can be observed directly in real time.

While most cells show a uniform signal at the membrane (Figs. 4A and 4B), some structures concentrate the fusion protein. These structures are generally actin and/or membrane-rich, such as neuropil (Fig. 7) or the pseudopods (Figs. 11b and 11c) and leading edges (Figs. 4C and 5) of migrating cells. During oogenesis, the fusion protein can specifically label the polar follicle cells, allowing us to study their behavior in live egg chambers (Fig. 11). Our results show that the fusion protein is uniquely suited to observing the morphogenesis and function of a specific membrane structure, the border cell process (Fig. 11e). We believe this approach will be similarly useful for studying sensory organs, the CNS, epidermis, and other cell types in which membrane projections play an important role in differentiation.

GFP is especially suited to imaging embryos, since it is easier to observe them live than to fix and stain them. Coupled with time-lapse methods the GFP-moe allows a continuous read-out of dynamic cell shape changes and migrations. In preliminary studies with live *hs-GFP-moe* embryos, we have made time-lapse, laser-scanning confocal microscope recordings of cell sheet movements during dorsal closure that are otherwise extremely difficult to image. The series of images is consistent with the purse string model for dorsal closure that we proposed earlier (Young *et al.,* 1993) because the leading edge proceeds dorsally in a smooth front. We anticipate this approach will provide important new information on the mechanisms by which various mutations disrupt morphogenesis in dorsal closure and in other morphogenic movements that contribute to the development of the fly.

ACKNOWLEDGMENTS

We thank K. Eilertsen and F. Schachat for assistance with the experiment shown in Fig. 2, Drs. Terry Oas and Jane Richardson for their advice on algorithms that predict coiled coil structures from primary sequence data, and members of the Kiehart lab for their support and helpful discussions. This work was supported by NIH Grant GM33830, the March of Dimes, and NIH Predoctoral Fellowship GM07184 to K.A.E.

REFERENCES

Algrain, M., Turunen, O., Vaheri, A., Louvard, D., and Arpin, M. (1993). Ezrin contains cytoskeleton and membrane binding domains accounting for its proposed role as a membrane-cytoskeletal linker. *J. Cell Biol.* **120,** 129–139.

Amieva, M. R., and Furthmayr, H. (1995). Subcellular localization of moesin in dynamic filopodia, retraction fibers, and other structures involved in substrate exploration, attachment, and cell–cell contacts. *Exp. Cell Res.* **219,** 180–96.

Arpin, M., Algrain, M., and Louvard, D. (1994). Membrane–actin microfilament connections: An increasing diversity of players related to band 4.1. *Curr. Opin. Cell Biol.* **6,** 136–141.

Ashburner, M. (1989). ''*Drosophila:* A Laboratory Handbook.'' Cold Spring Harbor Laboratory Press, Cold Spring Harbor, NY.

Barthmaier, P., and Fyrberg, E. (1995). Monitoring development and pathology of *Drosophila* indirect flight muscles using green fluorescent protein. *Dev. Biol.* **169,** 770–774.

Berger, B., Wilson, D. B., Wolf, E., Tonchev, T., Milla, M., and Kim,

P. S. (1995). Predicting coiled coils by use of pairwise residue correlations. *Proc. Natl. Acad. Sci. USA* **92,** 8259–8263.

Berryman, M., Gary, R., and Bretscher, A. (1995). Ezrin oligomers are major cytoskeletal components of placental microvilli: A proposal for their involvement in cortical morphogenesis. *J. Cell Biol.* **131,** 1231–4122.

Brand, A. H., Manoukian, A. S., and Perrimon, N. (1994). Ectopic expression in *Drosophila. Methods Cell Biol.* **44,** 635–654.

Chalfie, M., Tu, Y., Euskirchen, G., Ward, W. W., and Prasher, D. C. (1994). Green fluorescent protein as a marker for gene expression. *Science* **263,** 802–805.

Cody, C. W., Prasher, D. C., Westler, W. M., Prendergast, F. G., and Ward, W. W. (1993). Chemical structure of the hexapeptide chromophore of the *Aequorea* green-fluorescent protein. *Biochemistry* **32,** 1212–1218.

Davis, I., Girdham, C. H., and O'Farrell, P. H. (1995). A nuclear GFP that marks nuclei in living *Drosophila* embryos: Maternal supply overcomes a delay in the appearance of zygotic fluorescence. *Dev. Biol.* **170,** 726–729.

Doyle, T., and Botstein, D. (1996). Movement of yeast cortical actin cytoskeleton visualized *in vivo. Proc. Natl. Acad. Sci. USA* **93,** 3886–3891.

Edwards, K. A., Montague, R. A., Shepard, S., Edgar, B. A., Erikson, R. L. and Kiehart, D. P. (1994). Identification of *Drosophila* cytoskeletal proteins by induction of abnormal cell shape in fission yeast. *Proc. Natl. Acad. Sci. USA* **91,** 4589–4593.

Edwards, K. A., and Kiehart, D. P. (1996). *Drosophila* nonmuscle myosin II has multiple essential roles in imaginal disc and egg chamber morphogenesis. *Development* **122,** 1499–1511.

Endow, S. A., and Komma, D. J. (1996). Centrosome and spindle function of the *Drosophila* Ncd microtubule motor visualized in live embryos using Ncd-GFP fusion proteins. *J. Cell Sci.* **109,** 2429–2442.

Franck, Z., Gary, R., and Bretscher, A. (1993). Moesin, like ezrin, colocalizes with actin in the cortical cytoskeleton in cultured cells, but its expression is more variable. *J. Cell Sci.* **105,** 219–231.

Furthmayr, H., Lankes, W., and Amieva, M. (1992). Moesin, a new cytoskeletal protein and constituent of filopodia: Its role in cellular functions. *Kidney Int.* **41,** 665–670.

Gary, R., and Bretscher, A. (1995). Ezrin self-association involves binding of an N-terminal domain to a normally masked C-terminal domain that includes the F-actin binding site. *Mol. Biol. Cell.* **6,** 1061–1075.

Golic, K. G., and Lindquist, S. (1989). The FLP recombinase of yeast catalyzes site-specific recombination in the *Drosophila* genome. *Cell* **59,** 499–509.

Henry, M. D., Gonzalez Agosti, C., and Solomon, F. (1995). Molecular dissection of radixin: Distinct and interdependent functions of the amino- and carboxy-terminal domains. *J. Cell Biol.* **129,** 1007–1022.

Kerrebrock, A. W., Moore, D. P., Wu, J. S., and Orr-Weaver, T. L. (1995). Mei-S332, a *Drosophila* protein required for sister-chromatid cohesion, can localize to meiotic centromere regions. *Cell* **83,** 247–256.

Kiehart, D. P., Montague, R. A., Rickoll, W. L., Foard, D., and Thomas, G. H. (1994). High-resolution microscopic methods for the analysis of cellular movements in *Drosophila* embryos. *Methods Cell Biol.* **44,** 507–532.

Krieg, J., and Hunter, T. (1992). Identification of the two major epidermal growth factor-induced tyrosine phosphorylation sites in the microvillar core protein ezrin. *J. Biol. Chem.* **267,** 19258–19265.

Lindsley, D. L., and Zimm, G. G. (1992). "The Genome of *Drosophila melanogaster.*" Academic Press, New York.

Lupas, A., Van Dyke, M., and Stock, J. (1991). Predicting coiled coils from protein sequences. *Science* **252,** 1162–1164.

Lutz, D. A., and Inoué, S. (1986). Techniques for observing living gametes and embryos. *Methods Cell Biol.* **27,** 89–110.

Mahajan-Miklos, S., and Cooley, L. (1994). Intercellular cytoplasm transport during *Drosophila* oogenesis. *Dev. Biol.* **165,** 336–351.

Margolis, J., and Spradling, A. (1995). Identification and behavior of epithelial stem cells in the *Drosophila* ovary. *Development* **121,** 3797–3807.

McCartney, B. M., and Fehon, R. G. (1996). Distinct cellular and subcellular patterns of expression imply distinct functions for the *Drosophila* homologues of moesin and the neurofibromatosis 2 tumor suppressor, merlin. *J. Cell Biol.* **133,** 843–852.

Micklem, D. R., Dasgupta, R., Elliott, H., Gergely, F., Davidson, C., Brand, A., Gonzalez-Reyes, A., and St. Johnston, D. (1997). The *mago nashi* gene is required for the polarisation of the oocyte and the formation of perpendicular axes in *Drosophila. Curr. Biol.* **7,** 468–478.

Montell, D. J., Rorth, P., and Spradling, A. C. (1992). *slow border cells,* a locus required for a developmentally regulated cell migration during oogenesis, encodes *Drosophila* C/EBP. *Cell* **71,** 51–62.

Morgan, N. S., Heintzelman, M. B., and Mooseker, M. S. (1995). Characterization of myosin-IA and myosin-IB, two unconventional myosins associated with the *Drosophila* brush border cytoskeleton. *Dev. Biol.* **172,** 51–71.

Nakamura, F., Amieva, M. R., and Furthmayr, H. (1995). Phosphorylation of threonine 558 in the carboxyl-terminal actin-binding domain of moesin by thrombin activation of human platelets. *J. Biol. Chem.* **270,** 31377–31385.

Oas, T., and Endow, S. (1994). Springs and hinges: Dynamic coiled coils and discontinuities. *Trends Biochem. Sci.* **19,** 51–54.

Plautz, J. D., Day, R. N., Dailey, G. M., Welsh, S. B., Hall, J. C., Halpain, S., and Kay, S. A. (1996). Green fluorescent protein and its derivatives as versatile markers for gene expression in living *Drosophila melanogaster,* plant and mammalian cells. *Gene* **173,** 83–87.

Potter, S. M., Wang, C.-M., Garrity, P. A., and Fraser, S. E. (1996). Intravital imaging of green fluorescent protein using two-photon laser-scanning microscopy. *Gene* **173,** 25–31.

Prasher, D. C., Eckenrode, V. K., Ward, W. W., Prendergast, F. G., and Cormier, M. J. (1992). Primary structure of the *Aequorea victoria* green-fluorescent protein. *Gene* **111,** 229–233.

Robertson, H. M., Preston, C. R., Phillis, R. W., Johnson-Schlitz, D. M., Benz, W. K., and Engels, W. R. (1988). A stable genomic source of P-element transposase in *Drosophila melanogaster. Genetics* **118,** 461–470.

Schneider, I., and Blumenthal, A. B. (1978). *Drosophila* cell and tissue culture. *In* "The Genetics and Biology of *Drosophila,*" Vol. 2a (M. Ashburner and T. R. F. Wright, Eds.), pp. 266–315. Academic Press, London.

Shiga, Y., Tanakamatakatsu, M., and Hayashi, S. (1996). A nuclear GFP beta-galactosidase fusion protein as a marker for morphogenesis in living *Drosophila. Dev. Growth Differ.* **38,** 99–106.

Spradling, A. C. (1993). Developmental genetics of oogenesis. *In* "The Development of *Drosophila melanogaster*" (M. Bate and A. Martinez-Arias, Eds.), pp. 1–70. Cold Spring Harbor Laboratory Press, Cold Spring Harbor, NY.

Steams, T. (1995). Green fluorescent protein. The green revolution. *Curr. Biol.* **5,** 262–264.

Thummel, C. S., and Pirotta, V. (1992). New pCaSpeR P element vectors. *Dros. Inf. Serv.* **71,** 150.

Tsukita, S., Oishi, K., Sato, N., Sagara, J., Kawai, A., and Tsukita, S. (1994). ERM family members as molecular linkers between the cell surface glycoprotein CD44 and actin-based cytoskeletons. *J. Cell Biol.* **126,** 391–401.

Turunen, O., Wahlstrom, T., and Vaheri, A. (1994). Ezrin has a COOH-terminal actin-binding site that is conserved in the ezrin protein family. *J. Cell Biol.* **126,** 1445–1453.

von Kalm, L., Fristrom, D., and Fristrom, J. (1995). The making of a fly leg: A model for epithelial morphogenesis. *BioEssays* **17,** 693–702.

Waddle, J. A., Karpova, T. S., Waterston, R. H., and Cooper, J. A. (1996). Movement of cortical actin patches in yeast. *J. Cell Biol.* **132,** 861–870.

Wang, S., and Hazelrigg, T. (1994). Implications for bcd mRNA localization from spatial distribution of exu protein in Drosophila oogenesis. *Nature* **369,** 400–403.

Westphal, M., Jungbluth, A., Heidecker, M., Mühlbauer, B., Heizer, C., Schwartz, J.-M., Marriott, G., and Gerisch, G. (1997). Microfilament dynamics during cell movement and chemotaxis monitored using a GFP-actin fusion protein. *Curr. Biol.* **7,** 176–183.

Wolff, T., and Ready, D. F. (1993). Pattern formation in the *Drosophila* retina. *In* ''The Development of *Drosophila melanogaster*'' (M. Bate and A. Martinez-Arias, Eds.), pp. 1277–1325. Cold Spring Harbor Laboratory Press, Cold Spring Harbor, NY.

Xu, T., and Rubin, G. M. (1993). Analysis of genetic mosaics in developing and adult *Drosophila* tissues. *Development* **117,** 1223–1237.

Yeh, E., Gustafson, K., and Boulianne, G. L. (1995). Green fluorescent protein as a vital marker and reporter of gene expression in *Drosophila. Proc. Natl. Acad. Sci. USA* **92,** 7036–7040.

Young, P. E., Richman, A. M., Ketchum, A. S., and Kiehart, D. P. (1993). Morphogenesis in *Drosophila* requires nonmuscle myosin heavy chain function. *Genes Dev.* **7,** 29–41.

Zarani, F. E., and Margaritis, L. H. (1986). The eggshell of *Drosophila melanogaster.* V. Structure and morphogenesis of the micropylar apparatus. *Can. J. Zool.* **64,** 2509–2519.

Received for publication May 28, 1997
Accepted August 6, 1997